Molecular Orbital Calculations on Polythiophenes Containing Heterocyclic Substituents: Effect of Structure on Electronic Transitions

S. Radhakrishnan, R. Parthasarathi, V. Subramanian, and N. Somanathan*

Central Leather Research Institute, Adyar, Chennai 600 020, India

Received: November 17, 2005; In Final Form: June 7, 2006

Molecular orbital calculations have been performed on thiophene oligomers bearing heterocyclic substituents at the third position in order to understand the interplay of effects such as the nature of substituent, skeletal substitution pattern, heteroatom identity, etc. on electronic transitions. The geometry optimization was carried out using the semiempirical AM1 method, and the electronic transitions predicted for the oligomers were extrapolated for polymers using an oligomeric approach. The experimentally determined optical transitions were found to follow the predicted trend of electronic transitions of monomers and polymers.

Introduction

Conjugated polymers are of considerable interest due to their luminescent and electrical properties. Among this relatively new class of materials, π-conjugated thiophene-based oligomers (nTs) and polymers (PTs) are prominent because of their chemical and electrochemical stability and ready functionalization.[1−3] In addition to their use as conducting components, these materials are currently under intense investigation for applications in thin film transistors, electroluminescent diodes, lasers, sensors, and photovoltaic cells.[4−8] Furthermore, new electron-transporting hole-blocking (ETHB) structures have recently been described[9,10] in the continuing search for more efficient polymeric light-emitting diodes (LEDs). The use of electron-deficient heterocyclic small molecules or polymers in a separate electron transport layer or as a blend component in conjunction with the emissive material has proven very useful in improving balanced injection and recombination in organic LEDs.[11] These additional layers may, however, cause inhomogeneity in the device due to phase separation and/or crystallization thus affecting the efficiency. Considerable work has gone into the design of emissive materials for single/double-layer devices.[12−14] The designed structures contain groups, which can function as ETHB structures and, apart from acting as electroemissive materials with enhanced emission efficiencies, are also useful in tuning the emission wavelength. Structure−property relationships, particularly those pertaining to optical properties of polythiophenes substituted with side chains that can enhance the number of electrons (ETHB function), are of interest because of their potential use in high-resolution, all-color polymeric LED-based displays.[15]

Part of the interest in organic (opto) electronics stems from the facile control and flexibility that organic synthetic methodology affords in functionalizing the (oligo-, poly-) thiophene core. By a judicious choice of functionality it is possible to fine-tune key optical, electronic, and electrooptical properties.[16] Electron-donating (alkyl, alkoxy, alkyl amino, etc.) or electron-withdrawing (−CHO, −CN, $-NO_2$, etc.) substituents can raise or lower the energies of the highest occupied molecular orbital (HOMO) and the lowest unoccupied molecular orbital (LUMO) relative to the unsubstituted system. This allows rational modulation of the molecular "band gap".[17, 18] Appending electron-withdrawing or -donating groups onto the heterocyclic skeleton also alters the redox and optical properties.[19−21] These modifications ultimately affect the charge transport characteristics of the bulk solid and also define the role that the emissive material can play in various device configurations. A fundamental challenge in the development of organic electronic materials is to establish reliable, instructive, and computationally efficient theoretical methodologies to predict the optical properties of new substances. The methodology should have high predictive accuracy of optical properties over wide ranges of molecular structures, compositions, and absorption energies.[22] The presently available computational modeling methods have increased the accuracy of molecular orbital (MO) methods, which can provide accurate estimates of molecular geometries, including dihedral angles and rotational barriers, dipole moments, as well as electronic structure properties such as electron affinity, ionization potential, and band gaps.[23,24] In recent years, the semiempirical Hartree−Fock (HF) INDO method has been used to compute the electronic structure of isolated molecules and the supermolecular systems made of dimers or larger molecular clusters. The choice of the INDO/S Hamiltonian is dictated by the fact that INDO calculations provide descriptions of the electron structure of isolated and interacting conjugated molecules. This is in excellent agreement with corresponding experimental data.[25] Semiempirical molecular orbital calculations (AM1 for structures, ZINDO for electronic transition energies) have proved to be suitable tools for the prediction of absorption and fluorescence properties of substituted carbostyrils.[26] Cornil et al. explored the singlet transition energies and relative oscillator strengths for unsubstituted oligo thiophenes by means of the intermediate neglect of differential overlap/single configuration−interaction (INDO/SCI) calculations.[27] Belletete et al. investigated the optical properties of fluorene−thiophene derivatives, a light-emitting polymer.[28] Their study evaluates the performance of ZINDO/s calculations to predict electronic transitions. The band gaps of the monomers and polymer were predicted using density functional theory methods, and the influence of the thiophene monomeric structures was correlated with the optical properties.[29] The theoretical methods were used to study the optical transitions of benzothiazole-substituted thiophenes, and this was then compared with the properties of synthesized

* Author to whom correspondence should be addressed. Phone: +91-44-2441-1630 Fax: +91-44-2491-1589. E-mail: nsomanathan@rediffmail.com.

10.1021/jp0566461 CCC: $33.50
Published on Web 07/04/2006

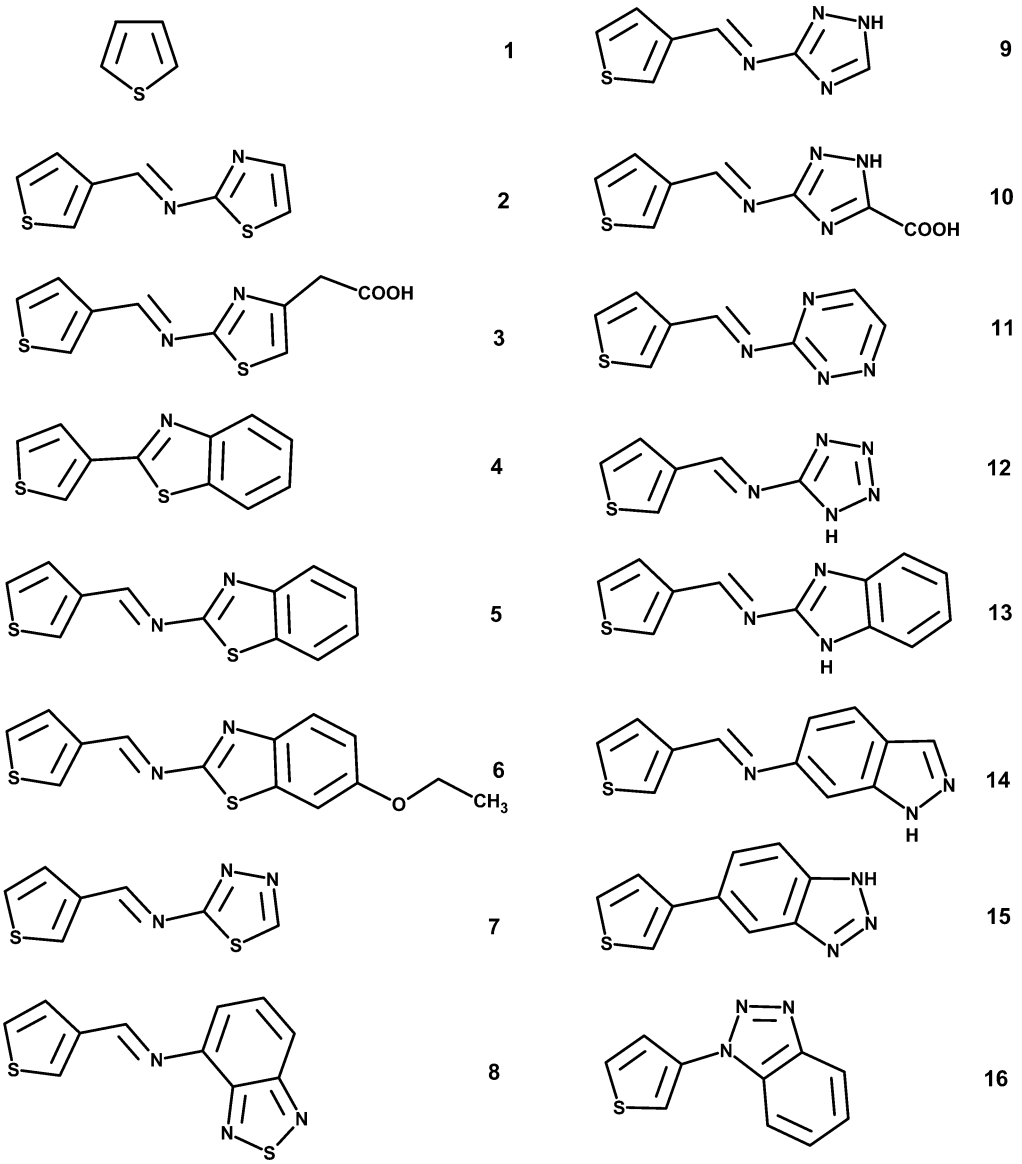

Figure 1. Different chemical structures of (a) group 1, (b) group 2, and (c) group 3.

polymers.[5] Similarly, the influence of the heteroatom and its position in the ring were also studied.[30]

Electronic transitions of novel polythiophenes are predicted on the basis of theoretical calculations. Our earlier studies[5,30] on the influence of structure on optical properties of 3-substituted thiophene monomers and polymers have shown the correlation of results obtained from theory with experimentally obtained results. To understand further, about 16 thiophene compounds containing hetero aromatic rings (containing highly electronegative sulfur and/or nitrogen in different positions (six- and five-membered fused rings)) as side chains attached to the 3-position of the thiophene rings were taken for a detailed study. The optical band gaps of the above compounds have been reported earlier.[29] The chemical structures of the monomers are shown in Figure 1. The theoretically obtained electronic transitions are correlated with the experimentally determined optical data.

Theoretical Methodology

The Cerius2 package from Accelrys has been used for generating the initial geometries, and the Gaussian 98W program[31] has been used for the semiempirical AM1 and ZINDO calculations. The geometries of the oligomers were optimized using the semiempirical AM1 Hamiltonian. ZINDO calculations were performed for geometries optimized from the AM1 calculation. For comparison, the parent thiophene oligomers (T) have also been optimized. In the ZINDO method, the first excited state with significant oscillator strength has been used for calculating the excitation energies. The geometrical characterizations have been extended to measure the torsion angles between adjacent thiophene rings and other substituents in the side chain. However, in some cases more transitions with comparable oscillator strengths are also used for comparison.

Synthesis of Monomers 2, 3, 5, 6, 7, 8, 9, 10, 11, 12, 13, and 14. The corresponding amine, dissolved in ethanol, was reacted with thiophene-3-carboxaldehyde in the presence of a catalytic amount of acetic acid. The mixture was refluxed for 1−6 h, and the resulting solid was filtered and washed with ethanol. The compound was purified by recrystallization.

Synthesis of Monomers 4 and 15. 3-Bromothiophene (0.01 mol) and magnesium turnings (0.01 mol) were introduced together with dry diethyl ether in a three-necked flask fitted with a condenser, a dropping funnel, and a nitrogen inlet. The entrainer 1,2-dibromoethane (0.01 mol) in anhydrous diethyl

ether was then added at ice-cold temperature for a period of 8 h. After the setting of the reaction, the solution was brought to ambient temperature. The resulting Grignard compound was transferred to a second dropping funnel fitted to a second three-necked flask containing 2-chlorobenzothiazole (0.01 mol) and 1,3- bis(diphenylphosphinopropane) nickel(II) chloride (Nidppp) in anhydrous diethyl ether. The Grignard compound was added dropwise at 0 °C, and the resulting adduct was allowed to warm to ambient temperature and stirred for 1 h. The contents were refluxed for 24 h. The obtained mixture was neutralized with very dilute aqueous hydrochloric acid. The organic layer was washed with water, dried, and concentrated. The crude product was purified on a silica gel column using petroleum ether (boiling range 60−80 °C) as the eluent.

Synthesis of Monomer 16. Monomer of **16** was prepared by microwave-assisted synthesis. The procedure followed for the synthesis is given below: Approximately 0.01 mol of 1H-benzotriazole was dissolved in 5 mL of chloroform. Approximately 0.01 mol of 3-bromothiophene was added to the above solution, and the chloroform solution was adsorbed in 20 g of silica gel (60−120 mesh). The silica gel was dried and subjected to microwave irradiation for 5 min. The maximum time of reaction and the microwave dosage were fixed on the basis of the study on the kinetics of the reaction. The obtained product was extracted with chloroform and further treated with 1% very dilute hydrochloric acid to remove the unreacted amine. The organic layer was washed with water, dried over anhydrous sodium sulfate, and purified further with column chromatography. The structure of the monomers was confirmed using NMR and IR spectroscopy. The results obtained are presented below.

Monomer 2. IR (cm^{-1}): 3100, 2943, 2857, 1605, 1513, 1447, 1412, 1321, 1148, 1074, 867, 834, 764, 692, 613. ^1H NMR (300 MHz, DMSO, ppm): 8.56 (d, 1H), 8.31 (d, 1H), 8.27 (s, 1H), 7.38 (m, 1H), 7.08 (m, 2H). ^{13}C NMR (75 MHz, DMSO, ppm): 157, 143.2, 139.5, 127.5, 126.9, 122.5, 122.4, 107.6.

Monomer 3. IR (cm^{-1}): 3099, 2948, 2915, 1604, 1519, 1413, 1376, 1319, 1147, 957, 867, 837, 787, 756, 693, 638. ^1H NMR (300 MHz, $CDCl_3$, ppm): 9.92 (s, 1H), 8.81 (s, 1H), 8.08 (s, 1H), 7.35 (m, 1H), 7.18 (m, 2H), 3.86 (s, 2H). ^{13}C NMR (75 MHz, $CDCl_3$, ppm): 165, 157, 143.8, 143.4, 133, 127.7, 126, 123.7, 122.1, 36.

Monomer 4. IR (cm^{-1}): 3087, 3057, 1588, 1539, 1477, 1432, 1398, 1373, 1312, 1240, 1184, 1123, 1074, 993, 943, 893, 870, 838, 786, 765, 730, 689, 653, 588, 436. ^1H NMR (300 MHz, $CDCl_3$, ppm): 8.02 (t, 2H), 7.85 (d, 1H), 7.69 (d, 1H), 7.39 (m, 3H). ^{13}C NMR (75 MHz, $CDCl_3$, ppm): 162.6, 153.8, 135.9, 134.6, 126.8, 126.5, 126.2, 126.0, 125.0, 123.0, 121.5.

Monomer 5. IR (cm^{-1}): 3096, 3062, 2949, 2847, 1602, 1538, 1446, 1412, 1309, 1261, 1218, 1162, 1101, 1016, 936, 884, 840, 789, 749, 691,623, 577, 473, 430. ^1H NMR (300 MHz, DMSO, ppm): 9.14 (s, 1H), {[7.84 (d), 7.76 (s), 7.61 (d), 7.39 (m), 7.18 (t)], 7H}. ^{13}C NMR (75 MHz, DMSO, ppm): 164.60, 161.07, 152.11, 141.08, 130.61, 128.48, 126.67, 125.52, 122.87, 121.29, 120.95, 118.52.

Monomer 6. IR (cm^{-1}): 3083, 2973, 2923, 2857, 1604, 1519, 1449, 1390, 1333, 1261, 1221, 1121, 1051, 943, 905, 869, 821, 795, 710, 681, 645, 586, 526. ^1H NMR (300 MHz, $CDCl_3$, ppm): 8.91 (s, 1H), {[7.96 (s), 7.82 (d), 7.72 (d)], 3H}, {[7.36 (t), 7.21 (d), 7.03 (dd)], 3H}, 4.03 (q, 2H), 1.42 (t, 3H). ^{13}C NMR (75 MHz, $CDCl_3$, ppm): 169.14, 158.32, 156.83, 145.80, 139.42, 135.51, 133.77, 126.97, 126.10, 123.45, 115.84, 104.91, 63.89, 14.65.

Monomer 7. IR (cm^{-1}): 3098, 1611, 1556, 1497, 1403, 1295, 1262, 886, 836, 773, 743, 615. ^1H NMR (300 MHz, DMSO, ppm): 8.57 (s, 1H), 8.30 (s, 1H), 7.39 (m, 1H), 7.16 (m, 2H). ^{13}C NMR (75 MHz, DMSO, ppm): 154.0, 151.7, 138.0, 128.0, 124.5, 122.5, 121.8.

Monomer 8. IR (cm^{-1}): 3087, 1607, 1442, 1335, 1198, 1107, 1078, 1022, 945, 892, 848, 783, 665, 609. ^1H NMR (300 MHz, $CDCl_3$, ppm): 8.11 (s, 1H), 7.89 (d, 1H), 7.78 (d, 1H), 7.38 (t, 1H), 7.31 (m, 1H), 7.22 (m, 2H). ^{13}C NMR (75 MHz, $CDCl_3$, ppm): 157.6, 155.9, 155, 148, 143.6, 137.6, 131.3, 129.9, 128.9, 125.6, 122.7.

Monomer 9. IR (cm^{-1}): 3111, 3049, 2940, 1604, 1483, 1331, 1169, 1027, 869, 832, 774, 693, 654, 614. ^1H NMR (300 MHz, DMSO, ppm): 8.56 (s, 1H), 8.05 (s, 1H), 7.45 (m, 1H), 7.02 (m, 2H). ^{13}C NMR (75 MHz, DMSO, ppm): 165, 154, 142, 140, 137, 128, 125.

Monomer 10. IR (cm^{-1}): 3105, 3046, 1598, 1483, 1421, 1339, 1168, 960, 831, 774, 694, 645, 615. ^1H NMR (300 MHz, DMSO, ppm): 8.26 (s, 1H), 7. 43 (m, 1H), 7.07 (m, 2H). ^{13}C NMR (75 MHz, DMSO, ppm): 160, 158, 154, 141, 140, 136, 128, 126.

Monomer 11. IR (cm^{-1}): 3101, 2854, 1603, 1558, 1529, 1489, 1327, 1116, 1075, 1046, 975, 863, 796, 653. ^1H NMR: (300 MHz, DMSO, ppm): 8.50 (d, 1H), 8.26 (s, 1H), 8.17 (d, 1H), 7.46 (m, 1H), 7.35 (m, 2H). ^{13}C NMR (75 MHz, DMSO, ppm): 153, 149, 145, 143, 140, 137, 134, 123.5.

Monomer 12. IR (cm^{-1}): 3099, 2919, 1602, 1588, 1546, 1508, 1412, 1235, 1100, 951, 840, 784. ^1H NMR (300 MHz, DMSO, ppm): 8.25 (s, 1H), 7.51 (m, 1H), 7.45 (m, 2H). ^{13}C NMR (75 MHz, DMSO, ppm): 157, 152, 149, 143, 129, 127.

Monomer 13. IR (cm^{-1}): 3044, 1598, 1520, 1495, 1436, 1401, 1278, 1240, 1192, 872, 834, 743, 610. ^1H NMR (300 MHz, DMSO, ppm): 8.28 (s, 1H), 7.69 (d, 2H), 7.66 (d, 2H), 7.46 (m, 1H), 7.39 (m, 2H). ^{13}C NMR (75 MHz, DMSO, ppm): 160.0, 156.5, 142.9, 140.3, 135.9, 134.8, 128.9, 125.8, 122.4, 119, 116, 103.

Monomer 14. IR (cm^{-1}): 3104, 2967, 2927, 1606, 1518, 1476, 1417, 1360, 1334, 1275, 1248, 1204, 1068, 846, 791, 701, 654. ^1H NMR (300 MHz, DMSO, ppm): 8.14 (s, 1H), 8.09 (m, 1H), 7.98 (m, 1H), 7.83 (m, 1H), 7. 69 (m, 1H), 7.33 (m, 1H), 7.2 (m, 2H). ^{13}C NMR (75 MHz, DMSO, ppm): 157, 156, 152.6, 149.5, 140.2, 127.7, 126.6, 125.8, 124.6, 121.7, 116.8, 104.2

Monomer 15. IR (cm^{-1}): 3280, 2970, 2880, 2362, 1782, 1663, 1606, 1529, 1474, 1387, 1322, 1245, 1169, 1112, 1068, 1037, 990, 838, 737, 630. ^1H NMR (300 MHz, $CDCl_3$, ppm): 7.29−7.27 (m, 3H), 7.17 (s, 1H), 7.02−6.96 (m, 2H). ^{13}C NMR (75 MHz, DMSO, ppm): 139, 136, 134, 129, 128, 125, 123, 117, 115.

Monomer 16. IR (cm^{-1}): 2924, 2854, 2366, 1960, 1740, 1596, 1461, 1212, 1113, 1015, 774, 746. ^1H NMR (300 MHz, $CDCl_3$, ppm): 7.96−7.94 (dd, 2H), 7.44−7.41 (dd, 2H), 7.27−7.03 (m, 1H), 7.02−6.8 (m, 2H). ^{13}C NMR (75 MHz, $CDCl_3$, ppm): 137.8, 129.0, 128.2, 126.9, 126.0, 125.3, 119.7, 118.0, 117.8, 115.0.

Electrochemical Polymerization. The electrochemical polymerization of Schiff bases was carried out in acetonitrile containing tetrabutylammonium hexafluorophosphate ($TBAPF_6$) as the electrolyte. The reaction was performed for 4 h with a current density of 1.43 mA/cm^2 for polymerization. Dedoping of the formed polymers was then carried out for 30 min by reversing the polarity. The procedure described above was adopted for synthesizing all the polymers. However, the absorption data taken for comparison for compounds **4, 5, 6,**

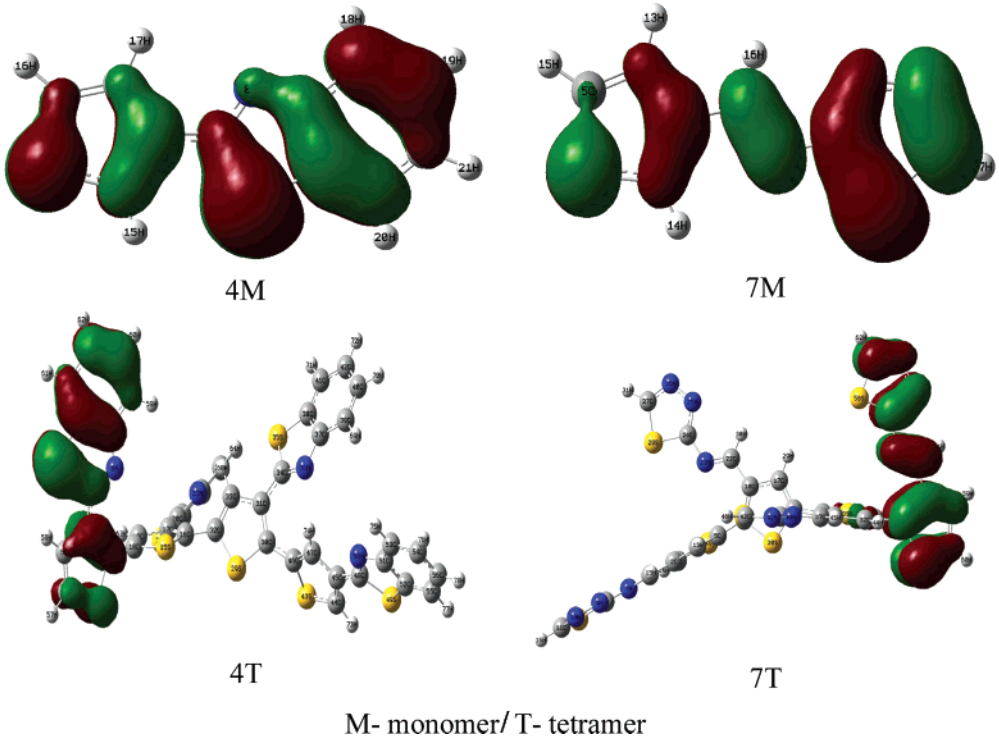

Figure 2. SOMO isosurfaces at 0.02 au for monomers of **4** and **7** and tetramers of **4** and **7**.

15, and **16** are from the chemically polymerized polymers (using $FeCl_3$ as the oxidizing agent).[5,30] The molecular weight (M_w) of the polymers is in the range of 8000−12 000 depending on the strain created in the molecule.

To analyze various coupling reactions of monomers, the singly occupied molecular orbitals (SOMOs) of radical cations of monomers and some oligomers have been studied at the semiempirical level using the AM1 Hamiltonian. The SOMO isosurfaces at 0.02 au for representative monomers of **4** and **7** and representative tetramers of **4** and **7** are depicted in Figure 2. Isosurfaces of SOMOs shows that electron density is not only delocalized on the thiophene ring but also on the benzothiazole ring. However, the isosurface of the SOMO for the tetramer reveals that it is more delocalized on the polymer propagation terminals. The SOMO features clearly reiterate that the coupling mode of the polymer is as expected from our theoretical observation. The IR spectral analysis of the polymers does not show any characteristic variation in coupling (polymerization) pattern and shows that the polymer is formed through thiophene ring of monomer units.

UV−Visible Absorption Spectral Analysis. The absorption spectra of the samples in methanol were recorded using the Cary UV-50-Bio UV−visible spectrophotometer. Thin films for the study were prepared from chloroform solution by coating the sample solution over quartz plates using a spin-coating technique.

Results and Discussion

A number of factors, including heteroatom identity, heterocyclic substituents, and conjugation length, are known to be important in obtaining the optical properties of conjugated organic oligomers and polymers. The electron-releasing or -withdrawing groups increase the HOMO or LUMO, respectively.[32] The energy of absorption decreases with alkyl substitution and decreases further with alkoxy substitution in polythiophenes. However, the situation is different with substitution at 3′-position of the 3-substituted thiophene. In this case, blue shift is observed irrespective of the change in substituent. Chemically polymerized poly(3,4-dimethylthiophene) is yellow, and poly(3,4-dibutoxythiophene) is green (λ_{max} = 460 nm), absorbing higher energy than their monofunctional analogues. Similarly poly(3-cyclohexylthiophene) emits green, while its methyl-substituted analogue poly(3-cyclohexyl-4-methylthiophene) emits in the blue region. The substitution at the 3,4-positions may lead to the predominant effect of steric hindrance along with the compromised electronic nature of the substituents.

Effect of Structure on Optical Transition: Group 1. To understand the role of substituents, the predicted electronic transition energies of monomers and polymers are compared in Figure 3. The compounds are ordered in idecreasing energy as shown below

monomers **4** > **8** > **5** > **6** > **2** > **3** > **7**

polymers **4** > **2** > **8** > **7** > **3** > **5**

With the analysis of the excitation energies of electronic transitions obtained from ZINDO calculations for the monomers of group 1, monomer **4** shows a high value (3.95 eV), and monomer **7** takes the low value of 3.23 eV. The lower value of monomer **7** can be attributed to the high extent of conjugation. In comparison to the benzothiazole side chain, benzothiadiazole has more π-bonds, leading to the red shift. In addition, resonance stabilization of the quinonoid structure may also be a contributing factor to the low transition energy.

It can be seen in Figure 1a that compounds **4**, **5**, and **6** have benzothiazole as a side chain, while in **5** and **6** the hetero aromatic ring is connected to thiophene through a azomethine linkage. At the monomer level, an additional π-conjugation may reflect red shift compared to that of monomer **4**. Steric effects are one of the major parameters influencing wavelength of absorption. The presence of direct linkage of a side chain viz. benzothiazole to the thiophene unit forces the molecule to take the sterically hindered geometry in **4.** Hence, the theoretically obtained absorption maxima are found to be very high compared

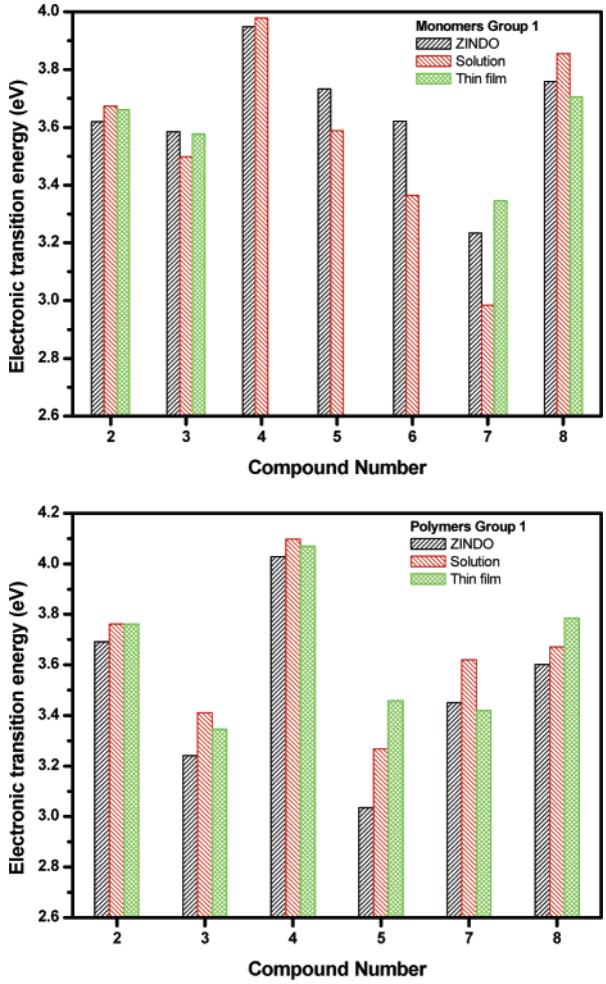

Figure 3. Comparison of electronic transition energies obtained by theory and experiments for monomers and polymers of group 1.

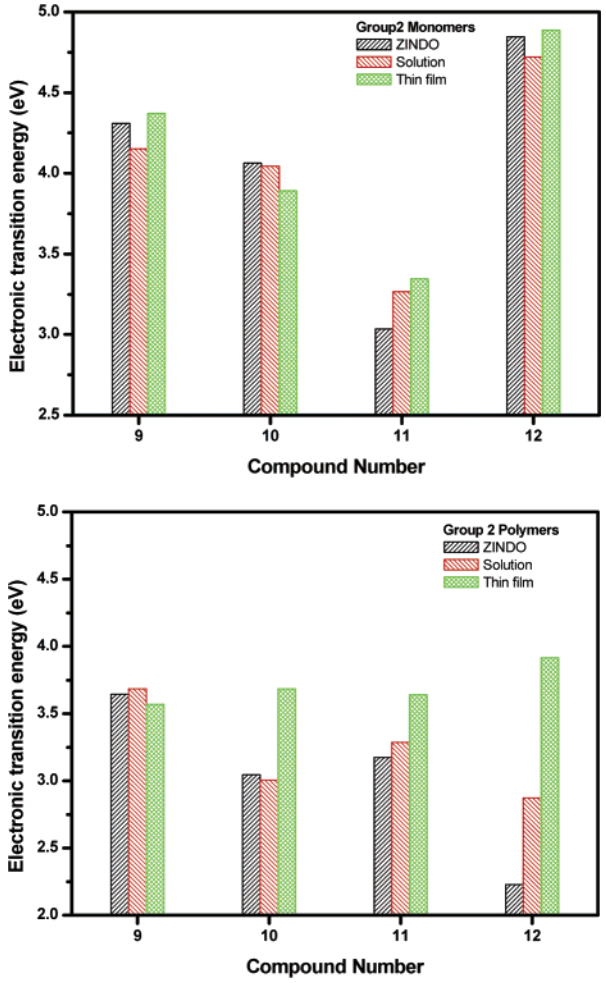

Figure 4. Comparison of electronic transition energies obtained by theory and experiments for monomers and polymers of group 2.

to those of other monomers of the same group. But the observed red shift in **6** compared to that of **5** is due to the substituent group ($-OC_2H_5$) attached to the benzothiazole group. In **3**, the presence of −COOH reduces the absorption energy compared to that of monomer **2**.

To understand the influence on photoabsorption of a specific functional group present in a side chain, the magnitudes of predicted values were compared with compounds having structural similarity. Even though monomers of both **4** and **5** have the same benzothiazole unit, in monomer **5,** benzothiazole is connected to the thiophene ring through a −CH═N linkage. Hence, the transition energy of monomer **4** is 5.4% higher than the transition energy of monomer **5.**

Although both monomers of **7** and **8** basically bear the thiadiazole group, due to the variation in linkage, when compared to monomer **8**, monomer **7** shows a red shift (14%) in transition energy. Monomer **6** shows a red shift of about 3% from the theoretically obtained value of monomer **5,** indicating the influence of electron-releasing $-OC_2H_5$ on absorption. Similarly, due to the influence of a $-CH_2COOH$ group, the transition energy of monomer **3** is red-shifted, when compared to that of monomer **2**.

The predicted transition energy for polymer **4** has a high value of 4.03 eV, while polymer **5** was found to have the lowest value of 3.03 eV. In comparison to other structures of group 1, polymer **4** continued to show a high band gap.[29] It has been reported that the dihedral angle and thus the π-orbital overlap between adjacent thiophene rings along the polymer backbone determine the effective conjugation length along the polymer chain.[15] In polymer **4**, the substituent benzothiazole may impose more steric hindrance to the main chain, leading to the large dihedral angle between the rings and short conjugation along the polymer backbone, which results in a higher blue-shifted transition energy value. Roncali et al. reported that the steric effects of the branched alkyl chain on the polymerization behavior are reduced when the thiophene ring is separated from a branched side chain with more than two carbon atoms.[33] Even though both polymer **4** and polymer **5** bear the benzothiazole side chain, the presence of a −CH═N− link may decrease the strain in polymer **5,** which, in turn, reduces the transition value for the same. Unsubstituted thiophene oligomers are effectively planar. and there is no regioregularity. But in the case of substituted thiophenes, the side chain play a vital role in deciding the planarity of the system by altering the inter-ring torsions. This may be the reason for the deviation order in polymers compared to that of monomers where there is no inter-ring torsion.

Effect of Structure on Optical Transition: Group 2. Nitrogen-based heterocycles have proved to be promising candidates for the charge transporting layer in organic LEDs.[34−37] In group 2, nitrogen-rich heterocyclic systems were chosen as side chains, and the influence of their structure on absorption was taken up for study. The predicted electronic transition energies of monomers and polymers are compared in Figure 4. Monomer **12** shows a maximum absorption of 4.85 eV, and monomer **11** exhibits the lowest absorption of about 3.03 eV.

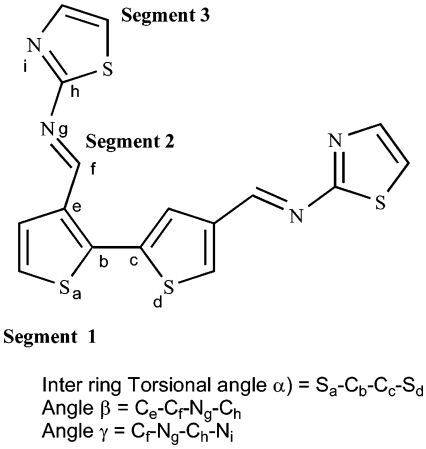

Figure 5. Representative figure showing different segments and angles used in this study.

Monomers and polymers of group 2 are ordered on the basis of predicted absorption energy as follows.

monomer **12** > **9** > **10** > **11**

polymer **9** > **11** > **10** > **12**

To have a better understanding, the optimized geometries and the torsion angles of different segments of the compounds were also considered for the discussion. The schematic representation of different torsional angles is presented in Figure 5. The optimized geometry of **12** shows torsion of about 53° (β) between segments 1 and 2 and about 94° (γ) is observed between segments 2 and 3. This may reduce the π-conjugation resulting in a high band gap for the respective case. A comparison of monomers **9** and **10** shows that segment 3 of **9** is twisted due to the presence of a COOH group, unlike in **10**, which has more planarity. Although **12** and **9** have five-membered rings (segment 3), the increase in the number of nitrogen atoms increases the energy of absorption in **12**. Both **9** and **11** contain the same number of nitrogen atoms, even though compound **9** contains a five-membered ring, whereas **11** has a six-membered ring. Thus the variation in properties in these compounds can be attributed to the ring size.

In the case of polymers, the extrapolated electronic transition energy results show that **9** and **12** have the highest and lowest values. An increase in the number of nitrogen atoms reduces the transition energy, as can be seen when the absorption energies of **9** and **12** are compared. The ring size as well as terminal substituent may influence the absorption.

Effect of Structure on Optical Transition: Group 3. Group 3 considers the benzo derivatives (fused rings) of nitrogen-based hetereocycle-substituted thiophenes to systematically understand the influence of steric and other effects of the structures on optical properties. Substituted polythiophenes containing electron-transporting groups such as benzotriazole or chlorobenzotriazole have been studied by Ahn et al.[38] In these studies benzotriazole was attached to the thiophene through ethyl groups, and this may reduce the strain of the molecule. The predicted electronic transition energies of monomers and polymers of the present study are compared in Figure 6. The decreasing orders of predicted absorption energy are

monomer **15** > **16** > **14** > **13**

polymer **15** > **16** > **13** > **14**

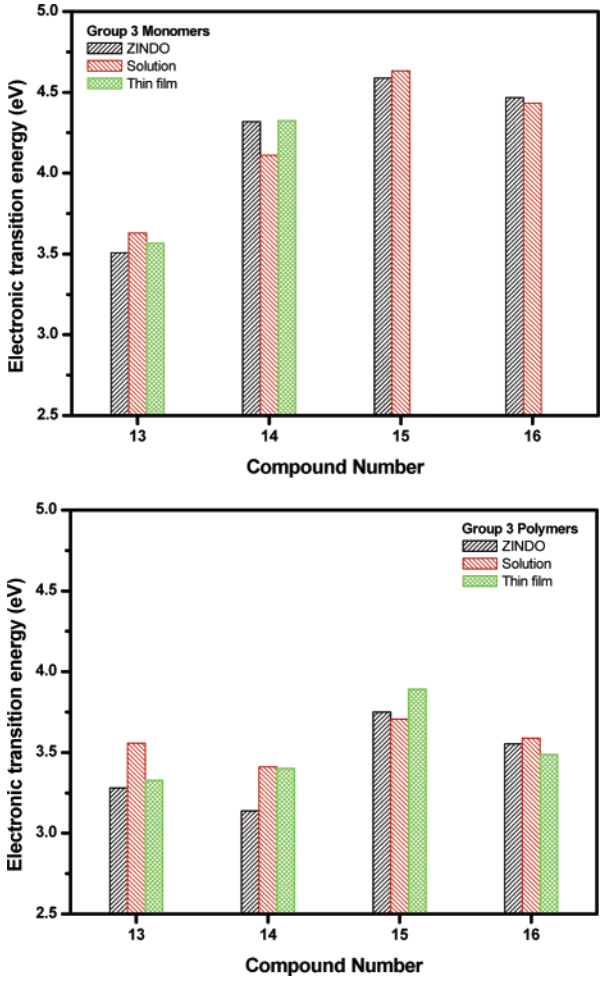

Figure 6. Comparison of electronic transition energies obtained by theory and experiments for monomers and polymers of group 3.

In group 3 monomers, **15** shows the highest transition energy of 4.59 eV, while **13** takes the lowest value of 3.51 eV. A high blue-shifted value is observed in both **15** and **16**, and this may be due to the direct linkage of the benzotriazole group linked to the thiophene ring. The azomethine linkage present in **13** and **14** additionally contributes to the extension of conjugation, leading to a red shift. There is a deviation of about 38° in the segment 3 (γ) of **14** unlike in **13**, which has a planar structure.

General Comparison of Polythiophenes Containing Heteroaromatic Side Chains. Thiophene-containing directly linked benzothiazole and benzotriazole substituents (**4**, **15**, and **16**) show extremely high blue-shifted values. In all these cases, the direct linkage produces steric hindrance in the molecule, and this is reflected in the blue shift in transition energies. In general, the steric influence dominates the absorption of these molecules to a larger extent rather than electronic effects.

Polymer **12** shows the lowest transition energy among the compounds taken for study. The polymers such as **11**, **5**, **13**, and **14** fall within this lower transition energy category. Here, the observed absorption is due to the compromised effect of both electronic and steric contributions. The presence of azomethine linkages contributes to the red shift.

Overall, the materials that absorb at the higher energy, all having high torsion angles, and their spatial distributions observed from their optimized geometries are also different from the geometries of the medium and low band gap materials. The representative geometries of some of the tetramers are shown in Figure 7.The optimized geometries of these strained molecules

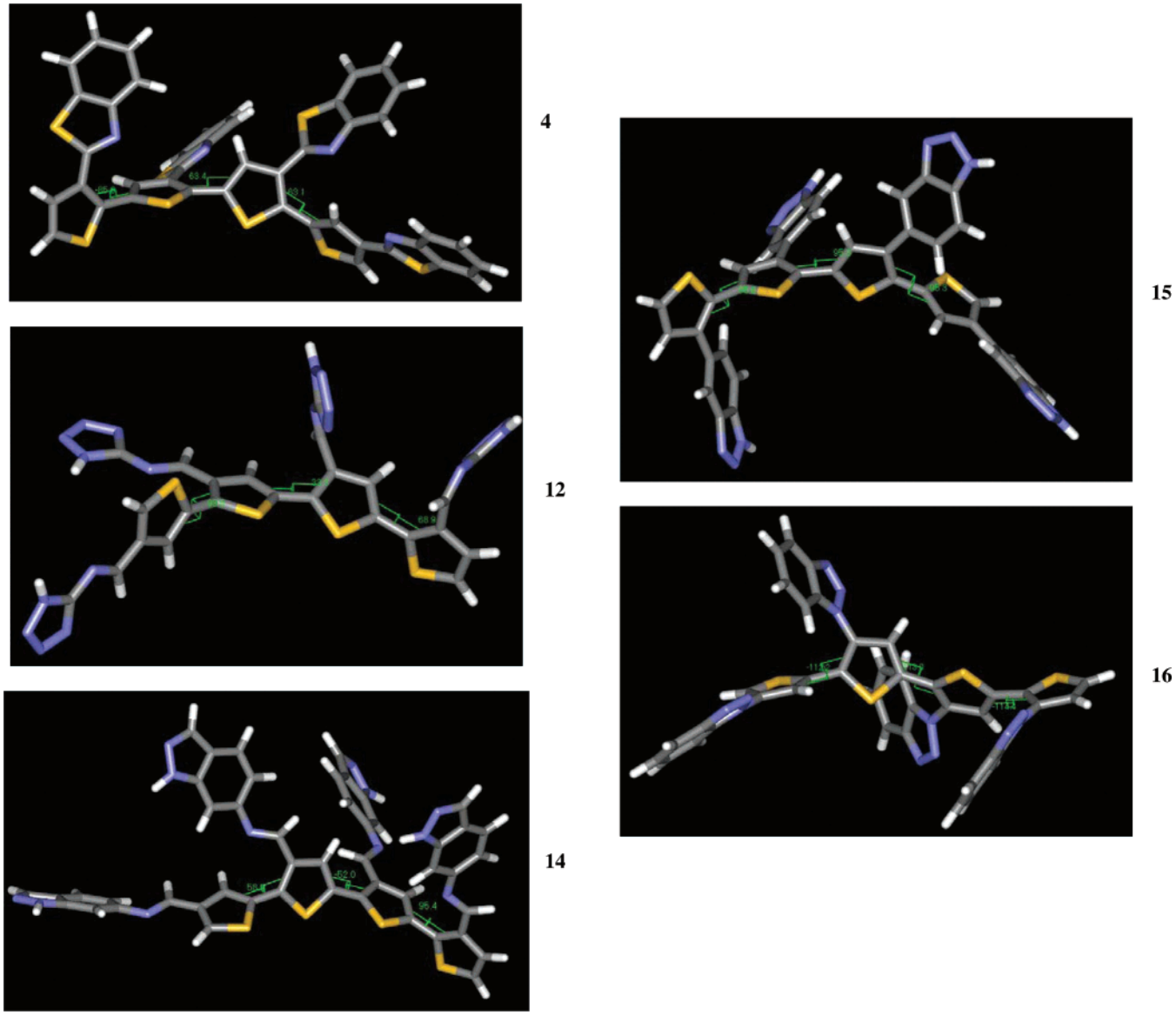

Figure 7. Optimized geometries of tetramers.

are found to distribute uniformly in space. The side views of the tetramers of **15** and **16** are shown in Figure 8, and the geometrical structures show that all thiophene units of tetramers fall on an axis and the side chains are evenly placed in an organized manner. This kind of three-dimensional packing may affect the formation of supramolecular architectures, which in turn modify its optical properties.

Comparison of Experimental and Theoretical Absorption Maxima. The peak values of experimentally determined absorption spectra (solution and thin films) of monomers and polymers of groups 1−3 were determined by analyzing the second derivatives of the experimentally determined spectra. The predicted transitions from ZINDO calculations are compared to the experimentally obtained absorption maxima (values in a comparable range with higher absorptivity are considered for comparison). The transitions with maximum oscillator strength in ZINDO results are considered for comparison with experimental results.

In Figure 3 the predicted (with ZINDO calculations) electronic transitions with maximum oscillator strengths and experimental λ_{max} values obtained in the same range (both solution and thin films) of group 1 monomers and polymers are compared. The predicted and experimentally observed transition energies are ordered in the sequence of decreasing energy. In monomers, both solution and thin film data follow the trend of theoretical results. However, the λ_{max} obtained from polymer thin films slightly deviates from experimental data. Thin film λ_{max} of polymer **3** shows deviation from the theoretical trend, perhaps due to the influence of solid-state packing. But in the case of polymer solution, the theoretically predicted trend is in exact agreement with the experimentally observed trend. Comparison of the order obtained in ZINDO calculations with the order from B3LYP/6-31G* (used for band gap calculations) shows that, excluding the position of **12**,[29] the order overlaps that for the monomers. Polymers of this group show a change in order especially with **3** and **5**. The bandwidth of the transition will also play a role in deciding the overall value. It is interesting to note that **3,** which has a carboxylic-acid-containing terminal group, has shown deviation in other properties too.

Experimental and predicted λ_{max} values of group 2 compounds are presented in Figure 4. The results show that the order of λ_{max} observed for monomers in solution and thin films are in good agreement with the predicted trend. But in the case of λ_{max} obtained from the polymer thin film, the reverse order of energy is observed. The energy-based ordering of compounds exactly matches the trend obtained in band gaps. In polymeric

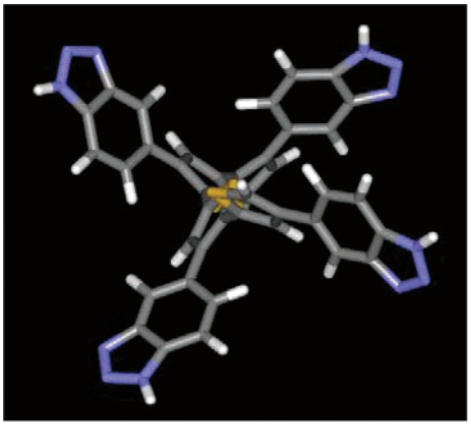

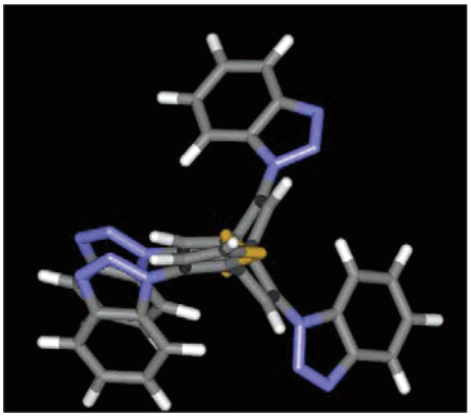

Figure 8. Optimized geometries of tetramers of **15** and **16** (side view).

thin films, **12**, which shows high deviation in band gap, changes the order of compounds.

In group 3, monomers and polymers, except in polymer thin film (Figure 6), the experimentally obtained values follow the same trend predicted by ZINDO. In the case of **15** and **16**, the predicted λ_{max} value shows an additional peak maximum with comparable oscillator strengths (3.81 eV in **15** and 3.95 eV in **16**). It is interesting to note that these additional peaks also overlap with the experimental data (3.81 eV).

Even though in some cases, a deviation in the theoretically obtained value from that of experimental values for solution and thin films is observed, overall transition energy results obtained using ZINDO show the validity of the method in predicting the transition energies. For example the transition energy values obtained for monomer **12** show an overlap with the experimentally obtained values. Whereas in the case of polymer **12**, the deviation of the experimental value from the theoretical value is high. Similarly, monomers **6** and **7** of group 1 and polymer **5** of group 1 show more deviation. To eliminate the influence of solvatochromism on transition energies (during comparison of structural influence on optical properties), the optical absorption spectra of the monomers and polymers are obtained in methanol solution, and the thin films of all monomers and polymers are prepared from chloroform solution. But depending on the type of aggregation of the compounds during thin film formation (H or J aggregation), the optical transition energy will change. The solvent used for the preparation of thin film also influences the type of aggregation. Depending on the polarity of the side chain in the monomer, the influence of solvatochromism will be different. In polymers, due to the polymerization of the thiophene rings, the polarity of the polymer is different from that of the monomer. Therefore the influence of solvent and on thin films may possibly bring more deviation from the theoretically obtained transition energy values.

The deviation in the trend of ZINDO results of polymer thin films can be attributed to the interactions involved in the polymeric chains apart from the parametrization of ZINDO. In general, ZINDO was parametrized on small molecules. For our purpose, the effectiveness of the computational method was determined both by the accuracy of the resulting transition energies and by the accuracy of the predicted oscillator strengths.[39] Further, the computed values from theoretical methods are in the gaseous phase, while the experimental values are obtained in solution, which may add some nonplanarity to the system.[24] In addition to solvent effects, electron correlation would also influence the transition energies calculated from molecular orbital calculations.

Conclusions

The comparison of theoretical and experimental results reveals the influence of the nature of sulfur/nitrogen-based heterocyclic side chains on optical properties of polythiophenes. It was shown that polythiophenes containing heterocyclic aromatic rings directly attached at the third position of thiophene ring exhibit highly blue-shifted electronic transitions. This is because of the higher degree of steric hindrance between bulky groups and the resultant twisting of the main chain and inhibition of π-stacking. The steric hindrance between the thiophene unit and side chain is relieved by the insertion of an azomethine group. The study finds its usefulness in predicting the electronic transitions and also in understanding the structure−property relationships of conjugated polymers.

References and Notes

(1) Frere, P.; Raimundo, J. M.; Blanchard, P.; Delaunay, J.; Richomme, P.; Sauvajol, J. L.; Orduna, J.; Garin J.; Roncali, J. *J. Org. Chem.* **2003**, *68*, 5357.
(2) Wang, J. Z.; Zheng, Z. H.; Li, H. W.; Huck W. T. S.; Sirringhaus, H. *Nat. Mater.* **2004**, *3*, 171.
(3) Afzali, A.; Breen T. L.; Kagan, C. R. *Chem. Mater.* **2002**, *14*, 1742.
(4) Kraft, A.; Grimsdale, A. C.; Holmes, A. B. *Angew. Chem., Int. Ed.* **1998**, *37*, 402.
(5) Mullen, K.; Wegner, G. *Electronic Materials: The Oligomer Approach*; Wiley-VCH: Weinheim, Germany, 1998.
(6) Pron, A.; Rannou, P. *Prog. Polym. Sci.* **2002**, *27*, 135.
(7) Andersson, M. R.; Thomas, O.; Mammo, W.; Svensson, M.; Theander, M.; Inganas, O. *J. Mater. Chem.* **1999**, *9*, 1933.
(8) Roncali, J. *J. Mater. Chem.* **1999**, *9*, 1875.
(9) Choy, W. C. H.; Hui, K. N.; Fong, H. H.; Liang, Y. J.; Chu, P. C. *Thin Solid Films* **2006**, *509*, 193.
(10) Liu, M. S.; Niu, Y. H., Luo, J.; Chen, B.; Kim, T. D.; Bardecker, J.; Jen, A. K. Y. *J. Macromol. Sci. Polym. Rev.* **2006**, *46*, 7.
(11) Thelakkat, M.; Schmidt, H. W. *Polym. Adv. Technol.* **1998**, *9*, 429.
(12) Jiang, X.; Burgoyne, W. F., Jr.; Robeson, L. M. *Polymer* **2006**, *47*, 4115.
(13) Forrest, S. R. *Org. Electron.* **2003**, *4*, 45.
(14) Radkahrishnan, S.; Subramanian, V.; Somanathan, N. *Org. Electron.* **2004**, *5*, 227.
(15) Akcelrud, L. *Prog. Polym. Sci.* **2003**, *28*, 875.
(16) *Handbook of Conductive Polymers*; Skotheim, T. A., Elsenbaumer, R. L., Reynolds, J. R., Eds.; Marcel Dekker: New York, 1998; pp 325−326.
(17) Casado, J.; Pappenfus, T. M.; Miller, L. L.; Mann, K. R.; Orti, E.; Viruela, P. M.; Pou-Amerigo, R.; Hernandez, V.; Lopez Navarrete, J. T. *J. Am. Chem. Soc.* **2003**, *125*, 2524.
(18) Moratti, S. C.; Cervini, R.; Holmes, A. B.; Baigent, D. R.; Friend, R. H.; Greenham, N. C.; Gruner, J.; Hamer, P. J. *Synth. Met.* **1995**, *71*, 2117.
(19) Casado, J.; Miller, L. L.; Mann, K. R.; Pappenfus, T. M.; Higuchi, H.; Orti, E.; Milian, B.; Pou-Amerigo, R.; Hernandez, V.; Lopez Navarrete, J. T. *J. Am. Chem. Soc.* **2002**, *124*, 12380.
(20) Lux, A.; Holmes, A. B.; Cervini, R.; Davies, J. E.; Moratti, S. C.; Gruner, J.; Cacialli, F.; Friend, R. H. *Synth. Met.* **1997**, *84*, 293.
(21) Bredas, J. *Adv. Mater.* **1995**, *7*, 263.

(22) Bredas, J. L. *Synth. Met.* **1997**, *84*, 3.
(23) Facchetti, A.; Yoon, M.; Stern, C. L.; Hutchison, G. R.; Ratner, M. A.; Marks, T. J. *J. Am. Chem. Soc.* **2004**, *126*, 13480.
(24) Kwon, O.; McKee, M. L. *J. Phys. Chem. A* **2000,** *104*, 7106.
(25) Janzen, D. E.; Burand, M. W.; Ewbank, P. C.; Pappenfus, T. M.; Higuchi, H.; da Silva Filho, D. A.; Young, V. G.; Bredas, J. L.; Mann, K. R. *J. Am. Chem. Soc.* **2004**, *126*, 15295.
(26) Fabian, W. M. F.; Niederreiter, K. S.; Uray G.; Stadlbauer, W. *J. Mol. Struct.* **1999**, *477*, 209.
(27) Cornil, J.; Beljonne, D.; Bredas, J. L. *J. Chem. Phys.* **1995**, *103*, 842.
(28) Belletete, M.; Beaupre, S.; Bouchard, J.; Blondin, P.; Leclerc, M.; Durocher, G. *J. Phys. Chem. B* **2000**, *104*, 9118.
(29) Radhakrishnan, S.; Parthasarathi, R.; Subramanian V.; Somanathan, N. *J. Chem. Phys.* **2005**, *123*, 164905.
(30) Radhakrishnan, S.; Parthasarathi, R.; Subramanian, V.; Somanathan, N.; *Comput. Mater. Sci.*, in press.
(31) Frisch, M. J.; Trucks, G. W.; Schlegel, H. B.; Scuseria, G. E.; Robb, M. A.; Cheeseman, J. R.; Zakrzewski, V. G.; Montgomery, J. A.; Stratmann, R. E.; Brant, J. C.; Dapprich, S.; Millam, J. M.; Daniels, A. D.; Kudin, K. N.; Strain, M. C.; Farkas, O.; Tomasi, J.; Barone, V.; Cossi, M.; Cammi, R.; Mennuci, B.; Pomelli, C.; Adamo, C.; Clifford, S.; Ochterski, J.; Pattersson, G. A.; Ayala, P. Y.; Cui, Q.; Morokuma, K.; Malick, D. K.; Rabuck, A. D.; Raghavachari, K.; Foresman, J. B.; Cioslowski, J.; Ortiz, J. V.; Stefanov, B. B.; Liu, G.; Liashenko, A.; Piskorz, P.; Komaromi, I.; Gomperts, R.; Martin, R. L.; Fox, D. J.; Keith, T.; Al-Laham, M. A.; Peng, C. Y.; Nanayakkara, A.; Gonzalez, C.; Challacombe, M.; Gill, P. M. W.; Johnson, B. G.; Chen, W.; Wong, M. W.; Andres, J. L.; Head-Gordon, M.; Replogle, E. S.; Pople, J. A. *Gaussian 98W*, revision A.1; Gaussian, Inc.: Pittsburgh, PA, 1998.
(32) Roncali, J. *Chem. Rev.* **1997**, *97*, 173.
(33) Roncali, J.; Garreau, R.; Yassar, A.; Marque, P.; Garnier, F.; Lemaire, M. *J. Phys. Chem.* **1987**, *91*, 6706.
(34) Yasuda, T.; Imase, T.; Sasaki S.; Yamamoto, T. *Macromolecules* **2005**, *38*, 1500.
(35) Ahn, S. H.; Ahn, T. K.; Han, S. H.; Lee, H. *Mol. Cryst. Liq. Cryst.* **2000**, *349*, 459.
(36) Promislow, J. H.; Preston, J.; Samulski, E. T. *Macromolecules* **1993**, *26*, 1793.
(37) Belmar, J.; Parra, M.; Zuniga, C.; Perez, C.; Munoz, C.; Omenat A.; Serrano, J. L. *Liq. Cryst.* **1999**, *26*, 389.
(38) Ahn, S. H.; Czae, M.; Kim, E. R.; Lee, H.; Ho Han, S.; Noh, J.; Hara, M. *Macromolecules* **2001**, *34*, 2522.
(39) Hutchison, G. R.; Ratner, M. A.; Marks, T. J. *J. Phys. Chem. A* **2002**, *106*, 1.